Chinese Chemical Letters 33 (2022) 1365–1372

Contents lists available at ScienceDirect

Chinese Chemical Letters

journal homepage: www.elsevier.com/locate/cclet

# "Small amount for multiple times" of $H_2O_2$ feeding way in $MoS_2$-$Fe_x$ heterogeneous fenton for enhancing sulfadiazine degradation

Zhuan Chen[a,b], Cheng Lian[a], Kai Huang[a], Jiahui Ji[a,b], Qingyun Yan[a,b], Jinlong Zhang[a,b], Mingyang Xing[a,b,*]

[a] Key Laboratory for Advanced Materials and Joint International Research Laboratory of Precision Chemistry and Molecular Engineering, Feringa Nobel Prize Scientist Joint Research Center, Frontiers Science Center for Materiobiology and Dynamic Chemistry, Institute of Fine Chemicals, School of Chemistry and Molecular Engineering, East China University of Science and Technology, Shanghai 200237, China
[b] Shanghai Engineering Research Center for Multi-media Environmental Catalysis and Resource Utilization, East China University of Science and Technology, Shanghai 200237, China

ARTICLE INFO

*Article history:*
Received 28 April 2021
Revised 24 June 2021
Accepted 5 August 2021
Available online 11 August 2021

*Keywords:*
Fenton reaction
Co-catalytic
Molybdenum sulfide
Hydrogen peroxide
Singlet oxygen

ABSTRACT

In recent years, $MoS_2$ catalyzed/cocatalyzed Fenton/Fenton-like systems have attracted wide attention in the field of pollution control, but there are few studies on the effect of $H_2O_2$ feeding way on the whole Fenton process. Here, we report a new type of composite catalyst ($MoS_2$-$Fe_x$) prepared in a simple way with highly dispersed iron to provide more active sites. $MoS_2$-$Fe_x$ was proved to possess selectivity for singlet oxygen ($^1O_2$) in effectively degrading sulfadiazine with a wide pH adaptability (4.0~10.0). Importantly, the mechanism of the interaction between $H_2O_2$ and $MoS_2$ on the Fenton reaction activity was revealed through the combination of experiment and density functional theory (DFT) calculations. Compared to the traditional "a large amount for one time" feeding way of $H_2O_2$, the "small amount for multiple times" of $H_2O_2$ feeding way can increase the degradation rate of sulfadiazine from 36.9% to 91.1% in the $MoS_2$-$Fe_x$ heterogeneous Fenton system. It is demonstrated that the "small amount for multiple times" of $H_2O_2$ feeding way can reduce the side reaction of decomposition of $H_2O_2$ by $MoS_2$ and effectively improve the utilization rate of $H_2O_2$ and the stability of $MoS_2$-$Fe_x$. Compared with $Fe_2O_3$-based Fenton system, $MoS_2$-$Fe_x$ can significantly save the amount of $H_2O_2$. Compared with nano-iron powder, the formation of iron sludge in $MoS_2$-$Fe_x$ system was significantly reduced. Furthermore, long-term degradation test showed that the $MoS_2$-$Fe_{75}$/$H_2O_2$ system could maintain the effectiveness of degrading organic pollutants for 10 days (or even longer). This study has a guiding significance for the large-scale treatment of industrial wastewater by improved Fenton technology in the future.



Due to the use of aromatic pollutants such as organic dyes, antibiotics and pesticides in various fields, these pollutants inevitably flow into natural groundwater, reservoir, and watercourse [1,2]. Water pollution caused by the disposal of sewage with pollutants above has become an environmental issue of great concern. So as to treat wastewater, physics, chemistry, biological treatment technologies are generally adopted, while advanced oxidation processes (AOPs) have attracted increasing interest as promising powerful methods to efficiently removing persistent organic pollutants from water [3–6]. Fenton or Fenton-like technology is one of the most important AOPs [7-9] and has been widely used in biology, environment and other fields. This type of technology relies on the generation of various reactive oxygen species (ROSs), such as hydroxyl radicals (·OH), singlet oxygen ($^1O_2$) and superoxide radicals ($\cdot O_2^-$) to degrade organic pollutants. However, practical Fenton technology used to degrade stable organic pollutants has certain drawbacks up to now. In the traditional Fenton reaction, $Fe^{3+}$ generated after $Fe^{2+}$ reacts with hydrogen peroxide ($H_2O_2$) cannot be recycled, which leads to the loss of iron source in the reaction and the reduction of Fenton reaction efficiency [10–12]. In addition, the opportune pH range in the conventional Fenton reaction is narrow [13]. High pH will make the generation of ROSs difficult and produce $Fe(OH)_3$ precipitation [14]. These objections severely hinder the further application of Fenton reaction.

To overcome the above shortages, in recent years, $MoS_2$ as a co-catalyst in Fenton reaction has attracted extensive concern since it can overcome most of the shortcomings of Fenton reactions. This is derived from the discovery by Xing *et al.* in 2018 [10]. They found that commercial 2H-type $MoS_2$ (< 2.00 μm) without any

* Corresponding author.
*E-mail address:* mingyangxing@ecust.edu.cn (M. Xing).

https://doi.org/10.1016/j.cclet.2021.08.016
1001-8417/

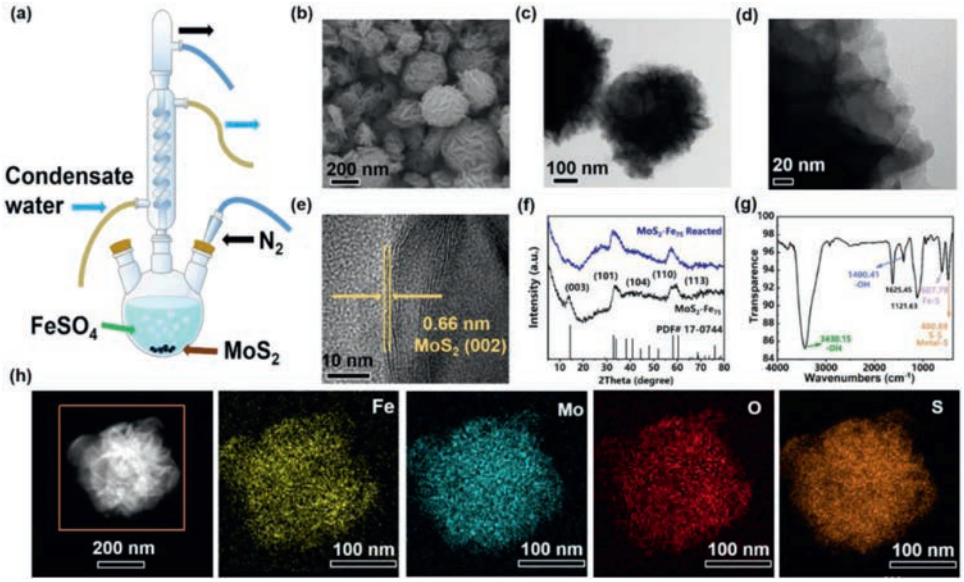


**Fig. 1.** Characterization of $MoS_2$-$Fe_{75}$. (a) The experimental device for preparing $MoS_2$-$Fe_{75}$. (b) SEM image of $MoS_2$-$Fe_{75}$. (c, d) TEM images of $MoS_2$-$Fe_{75}$. (e) HRTEM image of $MoS_2$-$Fe_{75}$. (f) XRD patterns of $MoS_2$-$Fe_{75}$ before and after reaction. (g) Infrared spectrum of $MoS_2$-$Fe_{75}$. (h) EDX mapping images of $MoS_2$-$Fe_{75}$.

additional treatment could serve as a cocatalyst to significantly accelerate the cycle of $Fe^{2+}/Fe^{3+}$ in Fenton reaction. Unsaturated S atoms on the surface of metal sulfides can capture protons from the solution to form $H_2S$, and expose reductive metallic active sites to greatly accelerate the rate-limiting step of $Fe^{3+}/Fe^{2+}$ conversion at the same time. In addition, the fast conversion of $Fe^{3+}/Fe^{2+}$ caused an increased amount of ·OH generated from the decomposition of $H_2O_2$, which was proved to rapid and efficient inactivate *Escherichia coli* K-12 (*E. coli*) and *Staphylococcus aureus* (*S. aureus*) [15]. In 2018, Xu *et al.* reported that flower-like $MoS_2$ powders were synthesized *via* a one-pot hydrothermal reaction and exhibited high-efficient adsorption performance to cationic dyes [16]. Due to strong electrostatic interaction between the positively charged pollutants molecules and electronegative $MoS_2$ nanoflowers, high-efficient adsorption capacity was very effective for improving the reaction efficiency of heterogeneous Fenton reaction. Next, Zhang *et al.* found that the performance of $MoS_2$ for activating $Fe^{3+}$/persulfate system can be effectively enhanced by introducing S defects into $MoS_2$ through thermal annealing. And the mechanism of S defects in accelerating the catalytic degradation of contaminants was revealed to be the modified surface charge distribution and enhanced adsorption of $Fe^{3+}$ [17]. Shen *et al.* developed a new and convenient biomimetic method to construct magnetic composites of $MoS_2$ and $Fe_3O_4$ magnetic nanoparticles ($MoS_2$-$Fe_3O_4$ MNPs) that effectively degraded methylene blue with $H_2O_2$ [18]. Indeed, it can be proved by current research that $MoS_2$ has a satisfactory effect in promoting the heterogeneous Fenton reaction, especially in solving the iron sludge problem and promoting the cycle of $Fe^{2+}/Fe^{3+}$. However, these researches tend to focus on designing more new catalysts based on $MoS_2$ to efficiently degrade pollutants in the different environment, while there are few studies on the effect of oxidant ($H_2O_2$ *etc.*)-$MoS_2$ interaction on the whole Fenton process. And the mechanics of the catalyst may have unexpected consequences for the whole Fenton reaction.

Herein, we reported a new type of easily prepared composite catalyst ($MoS_2$-$Fe_x$, x/mg represents the mass of $FeSO_4{\cdot}7H_2O$ in the precursor) by using $MoS_2$ as a co-catalyst while bringing its own highly dispersed iron source (Fig. 1a). The structure and composition of the catalysts were thoroughly analyzed with multiple characterization methods. Through the tests of transmission electron microscopy (TEM), high resolution TEM (HRTEM) and scanning TEM (STEM), it could be clearly seen that the $MoS_2$ still maintained the original nanoflower shape, and iron was evenly dispersed in the center and edge petals of the $MoS_2$ nanoflowers. Through the combination of experiments and DFT calculations, the mechanism of the interaction between $H_2O_2$ and $MoS_2$ on the activity of the whole Fenton system was explained, especially the feeding way of $H_2O_2$ played an important role. The sulfadiazine (SD) was used as a model pollutant to study the effect of the catalyst in the degradation of organic pollutants, and ROSs in the system were verified through electron paramagnetic resonance (EPR) and sacrificial agent experiments. It was found that the $MoS_2$-$Fe_x$ based Fenton system with a "small amount for multiple times" of $H_2O_2$ feeding way was suitable for treating organic pollutants in near neutral or even weakly alkaline environments. Finally, degradation experiments for other pollutants were used to prove the universality of the catalyst, and the stability of the catalyst was proved through cycle experiments and long-term experiments.

In order to investigate the specific morphology of the catalyst, scanning electron microscope (SEM) and TEM were used first to characterize the morphology and structure of $MoS_2$-$Fe_x$. It can be clearly seen from Figs. 1b and c that $MoS_2$-$Fe_{75}$ still maintained the nanoflower shape of $MoS_2$ with an average diameter of 0.10-0.60 μm and massive petals. According to the results of inductively coupled plasma atomic emission spectrometry (ICP-AES) in Table S1 (Supporting information), the iron content in the catalyst was about 13.0%. As shown in Fig. 1d, Figs. S1a and b (Supporting information), no particles were observed at the edge thin layer of $MoS_2$-$Fe_{75}$ nanoflowers in the TEM image, differing from three-dimensional (3D) $\alpha$-$Fe_2O_3$/$MoS_2$ hierarchical nano-heterostructure [19]. In the HRTEM images (Fig. 1e, Figs. S1c and d in Supporting information), only the lattice fringes of $MoS_2$ with low crystallinity were observed, which means that there was no crystalline iron or iron oxide embedded in $MoS_2$. In addition, the X-ray diffraction (XRD) pattern in Fig. 1f evidently showed the characteristic peaks of $MoS_2$ at $2\theta$ of 14.53°, 33.02°, 34.06°, 38.37°, 41.10°, 58.31° and 60.50°correspond well to $MoS_2$ Bragg planes of (003), (101), (012), (104), (015), (110) and (113), respectively. No characteristic peak of iron or iron oxides was observed, which was consistent with the result in the above HRTEM images. Although the content of Fe is as high as 13%, it does not generate any iron oxide, indicating that our synthesis strategy can achieve a highly dispersion of Fe atoms

on the $MoS_2$ surface. The XRD pattern of $MoS_2$-$Fe_{75}$ after reaction in Fig. 1f retained the characteristic peaks of $MoS_2$, which meant good stability of $MoS_2$-$Fe_{75}$.

On the basis of infrared spectrum of $MoS_2$-$Fe_{75}$ in Fig. 1g, the peaks at 3430.15 $cm^{-1}$ and 1400.41 $cm^{-1}$ indicated the presence of –OH on the surface of $MoS_2$-$Fe_{75}$. Compared with the infrared spectrum of $MoS_2$ in Fig. S2a (Supporting information), the peak at 3434.33 $cm^{-1}$ was significantly enhanced, which indicated that the introduction of iron brought more surface hydroxyl groups (–OH). Therefore, it could be speculated that some of the iron atoms in the catalyst were connected to the –OH during the preparation process. The peak at 607.79 $cm^{-1}$ indicated the stretching vibration of Fe–S bond [20], which illustrated that $Fe^{2+}$ was firstly coordinated with unsaturated S and then reduced and fixed on the surface of $MoS_2$, and it also explained why there was only a small peak belonging to $Fe^0$ in the followed high resolution X-ray photoelectron spectroscopy (XPS) results. Besides, the peak at 480.69 $cm^{-1}$ indicated the presence of Metal–S or S–S bond [21]. According to the infrared spectrum of $MoS_2$-$Fe_{75}$ after degradation reaction (Fig. S2b in Supporting information), the –OH of $MoS_2$-$Fe_{75}$ was reduced, proving that the –OH on its surface would be consumed with the dissolution of iron. In addition, the infrared spectrum of $TiO_2$-$Fe_{75}$ (Fig. S2c in Supporting information) confirmed that the introduction of Fe in the same way also resulted in a large number of surface –OH and further improved the hydrophilicity of the catalyst. According to Fig. S3 (Supporting information), nitrogen adsorption and desorption isotherms of $MoS_2$ and $MoS_2$-$Fe_{75}$ show that their specific surface areas were 29.9572 $m^2/g$ and 19.4070 $m^2/g$ respectively, accompanied by the hysteresis loop caused by nano petals. With the introduction of iron, the specific surface area of the catalyst was slightly reduced.

During the preparation process, $Fe^{2+}$ was more easily coordinated with unsaturated S on the surface of $MoS_2$ [17], leading to good dispersion and adhesion on the surface of $MoS_2$. With the addition of $NaBH_4$, $Fe^{2+}$ was reduced gradually. $MoS_2$-$Fe_x$ were also analyzed using STEM coupled with energy dispersive X-ray spectroscopy (EDX) to confirm the composition of catalyst. The corresponding EDX mapping images of $MoS_2$-$Fe_{75}$ in Fig. 1h showed that the homogeneous distribution of Fe (indicated by yellow color), Mo (indicated by blue color), O (indicated by red color) and S (indicated by orange color) elements, demonstrating the uniform distribution of Fe atoms among the whole $MoS_2$ nanoflower.

In order to investigate the effect of $MoS_2$-$Fe_x$ in the degradation of organic pollutants, we firstly tested the catalytic effect of $MoS_2$-$Fe_x$ prepared with different $FeSO_4{\cdot}7H_2O$ content in the precursor. When the mass of $FeSO_4{\cdot}7H_2O$ in the precursor was 75.0 mg, the catalytic effect of $MoS_2$-$Fe_x$ was the best (Fig. S4a in Supporting information). During the exploration, it was found that the addition of a large amount of $H_2O_2$ at one time did not achieve a good effect on the degradation of SD. According to the results in Fig. 2a, when the amount of $H_2O_2$ was 1.0, 4.0, 10.0, 20.0 and 100.0 μL, the degradation rate reached 33.0%, 41.0%, 43.0%, 41.3% and 43.9%, respectively, which may be due to the presence of excessive $H_2O_2$ triggered a large number of competing reactions [22]. Therefore, a "small amount for multiple times" feeding way of $H_2O_2$ may achieve better degradation effect. When 1.0, 1.5, 2.0 and 3.0 μL of $H_2O_2$ was added for 3 times, the degradation efficiency of SD reached 48.6%, 53.5%, 60.0% and 50.6%, respectively (Fig. S4b in Supporting information). The time interval of adding $H_2O_2$ was also proved to affect the degradation efficiency. With the increase of the total amount of $H_2O_2$, the activity of $MoS_2$-$Fe_{75}$ for the degradation of SD increased first and then decreased, indicating that excessive $H_2O_2$ with $MoS_2$-$Fe_{75}$ as the catalyst inhibited the degradation process due to reaction between $MoS_2$ and $H_2O_2$. When the total amount of $H_2O_2$ is constant, the activity of the catalyst increases slightly with the increase of reaction time. For instance, the degradation rate of the $MoS_2$-$Fe_{75}$/1*6-60min (The Z/a*b-cmin means a μL of $H_2O_2$ was added to the solution every c/b min, a total of b times, and the total experiment time was c min with Z as catalyst) system was only 13.0% higher than that of the $MoS_2$-$Fe_{75}$/1*6-30min system (Fig. S4c in Supporting information). Interestingly, the feeding way of $H_2O_2$ has a significant effect on the Fenton activity of $MoS_2$-$Fe_x$. For example, when the total amount of $H_2O_2$ is fixed at 9.0 μL in $MoS_2$-$Fe_{75}$ based Fenton system, the degradation rate of the system adding $H_2O_2$ in 9 times is much higher than that of the system adding $H_2O_2$ in three or one time (Fig. S4c). In order to maximize the utilization rate of $H_2O_2$, a total of 9.0 μL $H_2O_2$ is added into the solution in 9 times (adding 1.0 μL $H_2O_2$ every 10 min), which is defined as $MoS_2$-$Fe_{75}$/1*9-90min under the optimal degradation condition for 10 mg/L of SD without adjusting pH here.

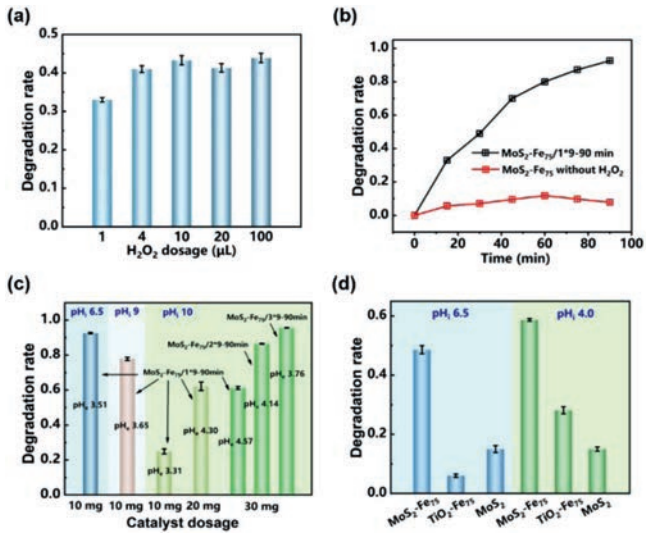


**Fig. 2.** Degradation rate of SD under different conditions with $MoS_2$-$Fe_{75}$. (a) Degradation rate at different dosages of $H_2O_2$ without adjusting pH ($H_2O_2$ is added at one time; SD: 10.0 mg/L, $MoS_2$-Fe75: 100.0 mg/L, Reaction time: 30 min). (b) Changes in degradation rate over time under optimal conditions (SD: 10.0 mg/L, $MoS_2$-$Fe_{75}$: 100.0 mg/L, $MoS_2$-$Fe_{75}$/1*9-90min, $pH_i$ 6.50). (c) The degradation of different dosages of catalyst and $H_2O_2$ under different pH ($pH_e$ means the pH value at the end of reaction). (d) The degradation efficiency of other catalysts prepared by the same method (SD: 10.0 mg/L, catalyst: 100.0 mg/L, $MoS_2$-$Fe_{75}$/1*3-30min).

In addition, $MoS_2$-$Fe_{75}$ exhibited interesting wide pH adaptability. When 10 mg of $MoS_2$-$Fe_{75}$ was added to 10 mg/L of SD solution, the initial pH ($pH_i$) of the solution was 6.5. As shown in Fig. 2b, $MoS_2$-$Fe_{75}$ based Fenton system showed much higher efficiency in degrading SD than the blank catalyst without $H_2O_2$. When the $pH_i$ of the $MoS_2$-$Fe_{75}$/1*9-90min system was close to neutral, the degradation rate was fast at first and then slowed down gradually. The degradation rate of the $MoS_2$-$Fe_{75}$/1*9-90min system can reach 93.2%, when the $pH_i$ is 6.50 (Fig. 2c). Even when the $pH_i$ was increased to 9.00, the degradation rate of the $MoS_2$-$Fe_{75}$/1*9-90min system remained at 77.9%. However, when the $pH_i$ was 10.0, its degradation rate could only reach 24.9%. To solve this problem, the addition amounts of $MoS_2$-$Fe_{75}$ and $H_2O_2$ were increased, as shown in Fig. 2c. Obviously, the degradation rate of the $MoS_2$-$Fe_{75}$/3*9-90min system could reach 95.6% with 300.0 mg/L $MoS_2$-$Fe_{75}$ added, indicating that the increase of the amount of $MoS_2$-$Fe_{75}$ and $H_2O_2$ had varying degrees of impact on the degradation rate. As shown in Fig. S4d (Supporting information), when $pH_i$ was 10.00, we also monitored the concentration of SD in the system in real time. Similar to the experiment of $pH_i$ 6.50, the concentration of SD in the system also decreased with each addition of $H_2O_2$ instead of waiting until the pH dropped to a certain level before it started to decrease. Although the pH of the system con-

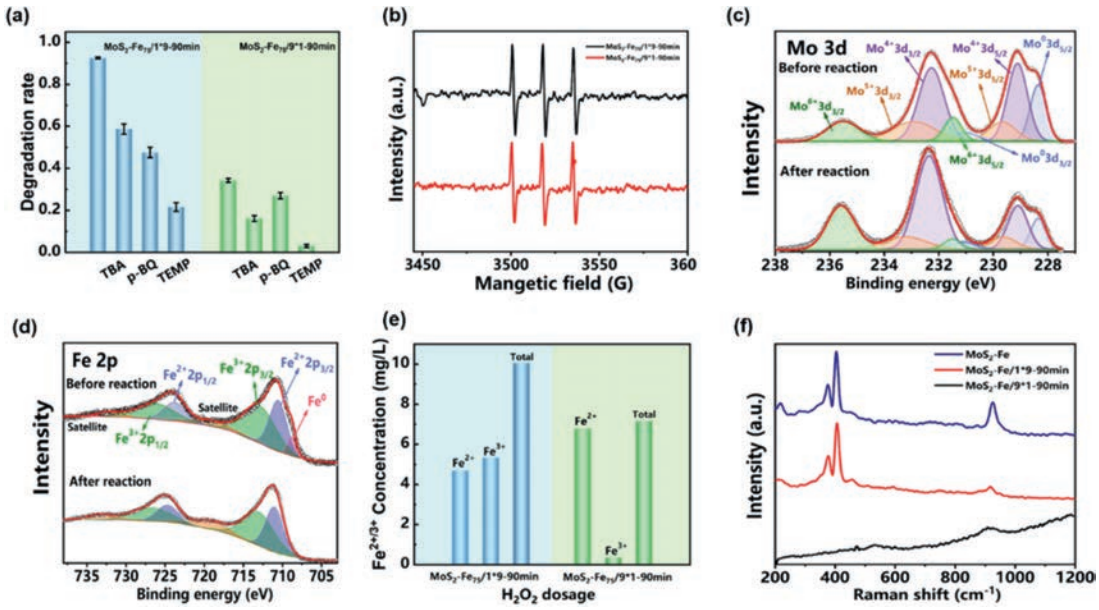


**Fig. 3.** Detection of ROSs in the system and changes in catalysts before and after the reaction. (a) Degradation rate of SD in the presence of different radical scavengers including TBA (0.02 mol/L), *p*-BQ (0.70 mmol/L), and TEMP (0.14 mmol/L) for the quenching of ·OH, $\cdot O_2^-$, and $^1O_2$, respectively, under the optimal conditions (SD: 10.0 mg/L, $MoS_2$-$Fe_{75}$: 100.0 mg/L, $MoS_2$-$Fe_{75}$/1*9-90min). (b) EPR spectra for the detection of $^1O_2$ in the presence of TEMP (98.0%, GC), using water as the solvent. The details of the EPR tests are as follows: capture agent was added into the reaction solution after the reaction started for 1 min, and the EPR test was performed after mixing the two solutions for 30 s. (c) The XPS pattern of Mo 3d before and after co-catalytic Fenton reaction (left to right: 235.5, 232.9, 232.2, 231.4, 231.0, 229.7, 229.1, 228.3 eV). (d) The XPS pattern of Fe 2p before and after co-catalytic Fenton reaction (left to right: 732.5, 726.7, 723.8, 718.8, 713.3, 710.6, 708.7 eV). (e) The concentration of the dissolved iron ions in the system of $MoS_2$-$Fe_{75}$/1*9-90min and $MoS_2$-$Fe_{75}$/1*9-90min ($pH_i$ 6.5). (f) Raman spectra of $MoS_2$-$Fe_{75}$ and $MoS_2$-$Fe_{75}$ after different $H_2O_2$ added in the way of $MoS_2$-$Fe_{75}$/1*9-90min and $MoS_2$-$Fe_{75}$/1*9-90min.

tinued to decrease with the addition of $H_2O_2$ and became less than 4.0 at the end of reaction ($pH_e$ < 4.0, Fig. S5 in Supporting information), the degradation of SD was carried out with each addition of $H_2O_2$ (Fig. 2b), rather than when the pH reached the appropriate range for the Fenton reaction. Besides, the degradation rate reached the fastest at the beginning of the experiment and gradually slowed down as the pH decreased. Therefore, the degradation rate had no obvious correlation with the pH of the system but connected with the concentration of SD in the system. As for $MoS_2$-$Fe_{75}$, adsorption was not the main factor leading to the reduction of SD content. According to Fig. 2b, $MoS_2$-$Fe_{75}$ reached the adsorption equilibrium for SD in about 1 h, and the adsorption amount was about 10.0% of the total.

The chemical interaction between $MoS_2$ and Fe was indispensable because independent $MoS_2$ or Fe was difficult to degrade SD effectively. As shown in Fig. 2d, the effect of $TiO_2$-$Fe_{75}$ synthesized by the same method as $MoS_2$-$Fe_{75}$ was only about half of $MoS_2$-$Fe_{75}$ when the $pH_i$ was 4.00, while $TiO_2$-$Fe_{75}$ had almost no effect when the $pH_i$ was 6.50. As for $MoS_2$, it was difficult to degrade SD with the addition of $H_2O_2$. The degradation rate of SD only reached 11.5%, no matter the $pH_i$ of the system was 4.00 or 6.50, and the degradation rate here was probably due to the adsorption of $MoS_2$ itself, according to the previous adsorption test of $MoS_2$-$Fe_{75}$ in Fig. 2b.

To further explore the oxidation mechanism of the $MoS_2$-$Fe_{75}$ catalytic Fenton reaction, radical quenching tests were conducted by using *tert*-butanol (TBA), *p*-benzoquinone (*p*-BQ) and 2,2,6,6-tetramethylplperldine (TEMP) as the corresponding sacrificial agents. According to Fig. 3a, the degradation rate of SD in the $MoS_2$-$Fe_{75}$/1*9-90min system decreased inordinately with the addition of sacrificial agents under optimal conditions. Therein, the addition of TEMP that could sacrifice $^1O_2$ reduced the degradation rate of SD to 21.6%, which meant that $^1O_2$ played the most crucial role in the reaction, and TBA and *p*-BQ also hindered the degradation in a minor way at the same time. There were the same results occurring in the $MoS_2$-$Fe_{75}$/9*1-90min system, demonstrating the similar oxidation mechanism. This indicates that the different adding ways of $H_2O_2$ may not change the decomposition process of $H_2O_2$, but only improve the decomposition efficiency of $H_2O_2$. Additionally, EPR test was employed to further detect the radicals present in the system with 5,5-dimethyl-1-pyrrolidine-*N*-oxide (DMPO) and TEMP as capture agents. Interestingly, the $MoS_2$-$Fe_{75}$ catalytic Fenton system exhibited obvious signal of $^1O_2$ (Fig. 3b), while the signals of ·OH and $\cdot O_2^-$ was not detected immensely shown in Fig. S6 (Supporting information) violating the traditional Fenton process. The electrostatic layer formed by the negative charge on $MoS_2$-$Fe_{75}$ surface greatly attracted iron ions and positively charged pollutants while non-electropositive substance like TEMP and DMPO cannot be adsorbed to the surface of $MoS_2$-$Fe_{75}$ very soon, which may greatly affect the capture of ·OH and $\cdot O_2^-$ that formed near the surface of $MoS_2$-$Fe_{75}$.

Additionally, methyl phenyl sulfoxide (PMSO) as a probe was employed to detected Fe(IV) in the reaction [23]. Fe(IV) is able to convert PMSO into its oxidation product ($PMSO_2$), markedly differing from the ·OH-induced products. Depending on the $\eta$ which is the molar ratio of $PMSO_2$ produced to PMSO lost (Eq. 1 and Fig. S7 in Supporting information), its value increased to 0.16 in the first 15 min, which meant that Fe(IV) was not the primary oxidative species generated in the $MoS_2$-$Fe_{75}$/$H_2O_2$ system at the beginning of experiment and it got higher as the reaction went on. Compared with the degradation process of SD catalyzed by $MoS_2$-$Fe_{75}$ (Fig. 2b), SD was degraded fast at the beginning of the reaction and the reaction rate was getting slower, which was just opposite of the changing trend of $\eta$. Therefore, Fe(IV) was not the primary oxidative species generated in the $MoS_2$-$Fe_{75}$/$H_2O_2$ system during the whole process.

$$\eta = \frac{\Delta PMSO_2}{\Delta PMSO} \quad (1)$$

The XPS spectra of Mo 3d and Fe 2p were employed to study the surface chemical state of $MoS_2$-$Fe_{75}$, as is shown in Figs. 3c and d. As for the $MoS_2$-$Fe_{75}$ before reaction, there were four kinds of molybdenum ions and three kinds of iron ions on the surface. Compared with the original $MoS_2$ in Fig. S8 (Supporting information), the $Mo^{5+}$ on the surface of the $MoS_2$ was significantly reduced, and replaced by $Mo^{4+}$. $Mo^0$ existed on the surface of $MoS_2$-$Fe_{75}$ after reduction while $Mo^{6+}$ was still found on $MoS_2$-$Fe_{75}$. Additionally, there was $Fe^0$, $Fe^{2+}$ and $Fe^{3+}$ on the surface of $MoS_2$-$Fe_{75}$, and $Fe^{2+}/Fe^{3+}$ occupied the majority among them (Fig. 3d). For the catalyst after the reaction, $Mo^0$ and $Mo^{4+}$ was greatly consumed while $Mo^{6+}$ increased evidently. For the Fe in the catalyst, $Fe^0$ was consumed while the other iron ions did not change significantly, suggesting that $Fe^0$ was involved in the decomposition of $H_2O_2$ by the Fenton reaction.

The concentration of $Fe^{2+}$ was measured by 1,10-orthophenanthroline as a probe, while $Fe^{3+}$ was reduced to $Fe^{2+}$ first and then tested to calculate the total iron ions in the solution. According to Fig. 3e, the concentration of iron ions (10.07 mg/L) in the $MoS_2$-$Fe_{75}$/1*9-90min system was higher than that in the $MoS_2$-$Fe_{75}$/9*1-90min system (7.17 mg/L). However, the ratio of $Fe^{3+}$ to $Fe^{2+}$ in the former was 1.13, much higher than that in the latter (0.053). It meant that more $Fe^{2+}$ participated in the Fenton reaction and then were oxidized to $Fe^{3+}$, which made the degradation efficient. In other words, since $H_2O_2$ is added to the reaction system in a "small amount for multiple times" feeding way, the $Fe^{2+}$ dissolved on the catalyst surface can decompose $H_2O_2$ more effectively, thus maintaining a stable iron cycle and keeping the ratio of $Fe^{3+}/Fe^{2+}$ at about 1.0. It was proved that excessive $H_2O_2$ added at one time did not speed up the process of Fenton reaction, which may be due to the direct reaction between $H_2O_2$ and $MoS_2$. The side reaction of excess $H_2O_2$ and $MoS_2$ made less amount of $H_2O_2$ involved in the Fenton reaction, resulting in a lower content of $Fe^{3+}$ in the system of $MoS_2$-$Fe_{75}$/9*1-90min. Therefore, it is particularly important to understand the interaction between $H_2O_2$ and $MoS_2$.

According to the above phenomena and analysis, the following mechanism can be inferred: $Fe^0$ had strong reducibility that can reduce $O_2$ to form $H_2O_2$ in acidic environment (Eq. 2) [24]. $MoS_2$-$Fe_{75}$ only contained a small section of $Fe^0$ so that it was difficult to generate a large amount of $H_2O_2$, and the consumption of $Fe^0$ cannot be avoided. Part of iron ions on the surface of $MoS_2$-$Fe_{75}$ was dissolved with the addition of $H_2O_2$ (Eq. 3). As shown in Fig. 3d, the peak of $Fe^0$ completely disappeared, and the peaks of other iron ions in $MoS_2$-$Fe_{75}$ did not changed greatly. For some iron ions dissolved in the system, classic Fenton reaction was bound to happen in the system (Eq. 4), and $Fe^{2+}$ could also reduce the $O_2$ in the solution to $\cdot O_2^-$ (Eq. 5). And the main ROS was still derived from $H_2O_2$ because the degradation rate did not have a great effect when the experiment was carried out in nitrogen atmosphere according to Fig. S9 (Supporting information). For the molybdenum ions of $MoS_2$-$Fe_{75}$, $Mo^{4+}$ vastly facilitated the cycle of $Fe^{2+}$ and $Fe^{3+}$ (Eq. 6) during the reaction, preventing the formation of iron sludge and part of $Mo^{4+}$ was oxidized to $Mo^{6+}$ (Eq. 6) at the same time, which could be proved by the change of peaks in Mo 3d spectra. $Mo^{6+}$ could be reduced to $Mo^{4+}$ by $H_2O_2$, and $O_2$ was produced meanwhile (Eq. 7). Moreover, $Mo^0$ on the surface of $MoS_2$-$Fe_{75}$ effectively quenched ·OH in the system and then generated $Mo^{4+}$ and $OH^-$ (Eq. 8 and Scheme 1), while part of the ·OH may further reacted with $H_2O_2$ to form $\cdot O_2H$ (Eq. 9) [25] and $H_2O$. $\cdot O_2H$ was likely to be converted into $\cdot O_2^-$ (Eq. 10) [26] with the departure of $H^+$. Finally, $Mo^{6+}$ was reacted with $\cdot O_2^-$ to form $^1O_2$ for further oxidation reactions (Eq. 11). Significantly, Mo° can effectively quench ·OH in the system after the reaction between $H_2O_2$ and $Fe^{2+}$ [27], and $Mo^{6+}$ on the surface fleetly oxidized the $\cdot O_2^-$ to $^1O_2$, which made it difficult to capture ·OH and $\cdot O_2^-$ in the EPR tests. Relatively, $^1O_2$ has a longer lifetime and it was easier to be captured in the $MoS_2$-$Fe_{75}/H_2O_2$ system.

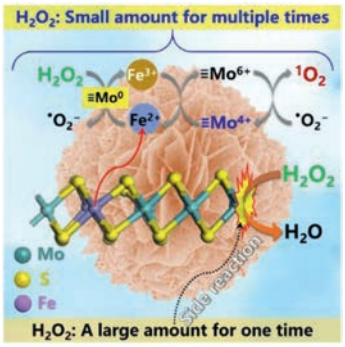


**Scheme 1.** Possible mechanism of $MoS_2$-$Fe_x$ for the decomposition of $H_2O_2$ in different feeding way.

$$Fe^0 + O_2 + H^+ \rightarrow Fe^{2+} + H_2O_2 \quad (2)$$

$$-S - Fe - OH + H^+ \rightarrow Fe^{2+} + H_2O + -S^- \quad (3)$$

$$Fe^{2+} + H_2O_2 \rightarrow Fe^{3+} + {}^{\bullet}OH + OH \quad (4)$$

$$Fe^{2+} + O_2 \rightleftharpoons Fe^{3+} + {}^{\bullet}O_2^- \quad (5)$$

$$Fe^{3+} + Mo^{4+} \rightarrow Fe^{2+} + Mo^{6+} \quad (6)$$

$$Mo^{6+} + H_2O_2 \rightarrow Mo^{4+} + O_2 + H_2O \quad (7)$$

$$Mo^0 + {}^{\bullet}OH \rightarrow Mo^{4+} + OH^- \quad (8)$$

$$^{\bullet}OH + H_2O_2 \rightarrow {}^{\bullet}O_2H + H_2O^- \quad (9)$$

$$^{\bullet}O_2H \rightleftharpoons H^+ + {}^{\bullet}O_2^- \quad (10)$$

$$Mo^{6+} + {}^{\bullet}O_2 \rightarrow Mo^{4+} + {}^1O_2 \quad (11)$$

As is known to all, traditional Fenton reaction is greatly limited by the narrow pH range. However, the degradation of SD in nearly neutral and alkaline was achieved effectively by using $MoS_2$-$Fe_{75}$ instead of $Fe^{2+}$ (Figs. 2b and c). High degradation rate was realized by increasing the amount of $MoS_2$-$Fe_{75}$ and $H_2O_2$, even though the catalytic performance of $MoS_2$-$Fe_{75}$ decreased at higher pH. Depending on the test in Fig. 2b, SD started to degrade immediately with the addition of $H_2O_2$, rather than when the pH of the solution became acidic. Therefore, high pH did not hinder the degradation in the $MoS_2$-$Fe_{75}/H_2O_2$ system, which may be attributed to the existence of acidic environment on the surface of $MoS_2$-$Fe_{75}$. As mentioned above, iron ions of $MoS_2$-$Fe_{75}$ was gradually dissolved with the addition of $H_2O_2$. Due to the existence of the unsaturated S with negative charges on the surface of $MoS_2$-$Fe_{75}$, $H^+$ and $Fe^{2+}$ tended to accumulate in the electrostatic layer near the surface of $MoS_2$-$Fe_{75}$, which constructed an acidic environment near the surface of $MoS_2$-$Fe_{75}$, and the pollutant was able to be degraded in this environment, so that the $MoS_2$-$Fe_{75}/H_2O_2$ system was no longer sensitive to pH.

Another interesting experimental phenomenon mentioned above was that compared with the addition of excessive $H_2O_2$ at once, the addition of $H_2O_2$ in batches with small amounts realized a better degradation effect. Fig. 3f exhibited the Raman spectra of $MoS_2$-$Fe_{75}$ before and after reaction. The $E_{2g}{}^1$ (384 $cm^{-1}$) and $A_{1g}$ (408 $cm^{-1}$) modes appeared at the same position as the commercial $MoS_2$. The peak at 930 $cm^{-1}$ was attributed to polymolybdates and its red shift [28] might be ascribed to the structure of –OH groups reported by Stencel *et al.* [29]. It was inferred that $MoS_2$ can instantly react with high concentration of $H_2O_2$ because the addition of $H_2O_2$ to the system in different ways had substantially different effects on $MoS_2$-$Fe_{75}$ (Scheme 1). As shown in Fig. 3f, the peak of $MoS_2$ was still prominent with $H_2O_2$ added in stages while barely seen with $H_2O_2$ added at one time. That means that $MoS_2$ of $MoS_2$-$Fe_{75}$ was greatly consumed in the $MoS_2$-$Fe_{75}$/9*1-90min system but maintained the original peaks in the $MoS_2$-$Fe_{75}$/1*9-90min system. Combined with the dissolution of iron ions in Fig. 3e, it can be concluded that most of the $H_2O_2$ may directly react with $MoS_2$ if the feeding rate of $H_2O_2$ was too fast, and the quick consumption of $H_2O_2$ made the Fenton reaction greatly restricted.

In addition, the prepared catalyst of $MoS_2$-$Fe_{75}$ was compared with the traditional heterogeneous Fenton catalysts, such as nano-iron powder (NIP) and $Fe_2O_3$. Interestingly, the experiment of NIP/9*1-90min got a degradability almost equivalent to $MoS_2$-$Fe_{75}$/1*9-90min while $Fe_2O_3$ could not be used to effectively degrade SD, as shown in Fig. 4a. In the system of $MoS_2$-$Fe_{75}$/1*9-90min, yellow iron mud was not found as is shown in Fig. S10 (Supporting information). However, it was easy for NIP/9*1-90min system to form a large amount of iron sludge after the reaction, causing considerable iron source loss (Fig. S11 in Supporting information). According to Fig. 4b, only a small amount of iron ions was left in the solution of NIP/9*1-90min system, and iron content in the yellow precipitate was very low, and more of precipitate was iron mud. In order to investigate the influence of $H_2O_2$ feeding way on $Fe_2O_3$ based heterogeneous Fenton system, we increased the amount of $H_2O_2$ to 63 μL to improve the degradation activity of the whole system, as shown in Fig. 4c. Unlike $MoS_2$-$Fe_{75}$ and NIP systems, $Fe_2O_3$ system is not sensitive to the feeding way of $H_2O_2$.The two feeding ways had no significant effect on the degradation activity of SD by $Fe_2O_3$ based Fenton system. The same phenomenon occurs in traditional homogeneous Fenton systems. When ferrous sulfate was used as the iron source, the activity of homogeneous Fenton reaction to degrade SD was also not affected by the feeding way of $H_2O_2$ (Fig. 4c). The above comparative experiments indicate that when researchers are developing new heterogeneous Fenton catalysts, they must consider the influence of $H_2O_2$ feeding way on the activity of the whole system. It is noted that $MoS_2$-$Fe_{75}$ can significantly reduce the amount of $H_2O_2$ compared with $Fe_2O_3$ based Fenton system; Compared with NIP, the formation of iron sludge was significantly reduced in $MoS_2$-$Fe_{75}$ system. Furthermore, the $MoS_2$-$Fe_{75}$ is fed with "small amount for multiple times" feeding way of $H_2O_2$, and its degradation activity is comparable to that of traditional homogeneous Fenton system.

To further understand the interaction between $H_2O_2$ and $MoS_2$, here, we have studied the adsorption of $H_2O_2$ on the surface of the catalyst by density functional theory (DFT) calculations. When the concentration of $H_2O_2$ is high, a large amount of $H_2O_2$ is close to the surface of $MoS_2$-$Fe_{75}$. At this time, the adsorption energy between the surface of $MoS_2$-$Fe_{75}$ and $H_2O_2$ cannot be calculated. In this case, a large amount of $H_2O_2$ will be decomposed into –OH and adsorbed on S atoms to form –S–O–H or –S–O, as shown in Figs. 4d and e. Therefore, only a small amount of $H_2O_2$ is decomposed to produce ROS, which also explains that in previous experiments, the $MoS_2$-$Fe_{75}$/9*1-90min system could not achieve a good degradation effect. However, when the concentration of $H_2O_2$ is low and its distance from the surface of $MoS_2$-$Fe_{75}$ is relatively far, different sites have different adsorption energies for $H_2O_2$. As shown in Figs. S12a and b (Supporting information) the adsorption energy of $H_2O_2$ on Mo site of $MoS_2$ is −1.643 eV, but it becomes smaller on Fe site (−1.112 eV) and on Mo site (−1.443 eV) of $MoS_2$-$Fe_{75}$, according to Figs. 4f and g. It means that the introduction of highly dispersed Fe weakens the adsorption of $MoS_2$ to $H_2O_2$ and reduces the amount of $H_2O_2$ that reacts directly with $MoS_2$ (Scheme 1), which also shows that the introduction of iron atoms improves the stability of $MoS_2$. Smaller absorption energy makes $H_2O_2$ dominant in the Fenton reaction when the amount of $H_2O_2$ is low. This point can also be confirmed in the iron dissolution experiment above (Fig. 3e). Compared with the one-time addition, more $Fe^{2+}$ are oxidize to $Fe^{3+}$ in the $MoS_2$-$Fe_{75}$/1*9-90min system, demonstrating that more $H_2O_2$ actually participate in the Fenton reaction when added in batches and lower concentration of $H_2O_2$ can better ensure the stability of $MoS_2$-$Fe_{75}$. There is still a big controversy as to whether the iron dissolved in the heterogeneous Fenton reaction or the iron in the solid phase plays a leading role [30]. According to the results of DFT calculations, the adsorption energy of $H_2O_2$ on Fe site of $MoS_2$-$Fe_x$ is smaller than that on Mo site, so $H_2O_2$ cannot directly react well with the iron in the solid phase of $MoS_2$-$Fe_{75}$. Therefore, it can be inferred that the iron dissolved on the catalyst surface is in the leading position in the Fenton reaction (Scheme 1).

In order to study the degradation pathway of SD in the $MoS_2$-$Fe_{75}$/$H_2O_2$ system, LC-MS/MS were used to determine the degradation intermediates. Sample was obtained through adding methanol when the $MoS_2$-$Fe_{75}$/1*9-90min system reacted for 10 min. The possible degradation intermediates are listed in Fig. S13 (Supporting information). Sixteen intermediates were identified, and a reasonable degradation pathway for SD by the $MoS_2$-$Fe_{75}$/$H_2O_2$ system was proposed. Due to the existence of sulfanyl and the pyrimidine ring in the SD, its degradation pathway was complicated. In the case of dominated by $^1O_2$, $C_3H_4O_4$ (*m/z* 103) and $C_2H_2O_4$ (*m/z* 90) occupied a large proportion of the product, which was mainly obtained by the ring-opening reaction of $C_{10}H_{10}N_4$ (*m/z* 187), $C_4H_5N_3$ (*m/z* 111) and $C_4H_4N_2$ (*m/z* 81) [31,32]. In addition, due to the good stability of the benzene ring, there were a large number of aromatic compound intermediates in the solution, such as $C_6H_5NO_3$ (*m/z* 139), $C_6H_7N$ (*m/z* 93), $C_6H_5NO_2$ (*m/z* 124). These intermediates were further mineralized in the following reaction. It's worth mentioning that ·OH in the traditional Fenton system will attack the amino group of SD to produce phenylhydroxylamine derivatives and other intermediates [33]. Phenylhydroxylamine derivatives are typical toxic byproducts, which can cause methemoglobinemia, and their toxicity is even higher than that of the SD molecule itself. However, in this case, the degradation pathways of SD based on $^1O_2$ produced by $MoS_2$-$Fe_{75}$/$H_2O_2$ system were significantly different. $^1O_2$ will directly attack the pyrimidine ring and the S–N bond, thus reducing the risk of forming phenylhydroxylamine toxic byproducts.

$MoS_2$-$Fe_{75}$ also exhibited excellent degradation performance on other model pollutants towards the removal of dyes and other antibiotics. Fig. 4h shows that the degradation rate of tetracycline hydrochloride, norfloxacin and enrofloxacin could reach 100.0%, 98.3% and 94.1% under the optimal degradation condition of SD. On the other hand, dyes such as new coccine, brilliant green, tartrazine and methyl orange were degraded in the system of $MoS_2$-$Fe_{75}$/1*3-30min and the degradation rates could reach 92.5%, 79.3%, 71.7% and 55.2%. This reflected that the $MoS_2$-$Fe_{75}$/$H_2O_2$ system had good degradability for different pollutants, which meant that this system had a certain degree of universality. As for the stability of $MoS_2$-$Fe_{75}$ during the degradation process, ten cycles of catalytic reaction tests were performed on the $MoS_2$-$Fe_{75}$/$H_2O_2$/RhB system under optimal conditions. As shown in Fig. 4i, the degra-

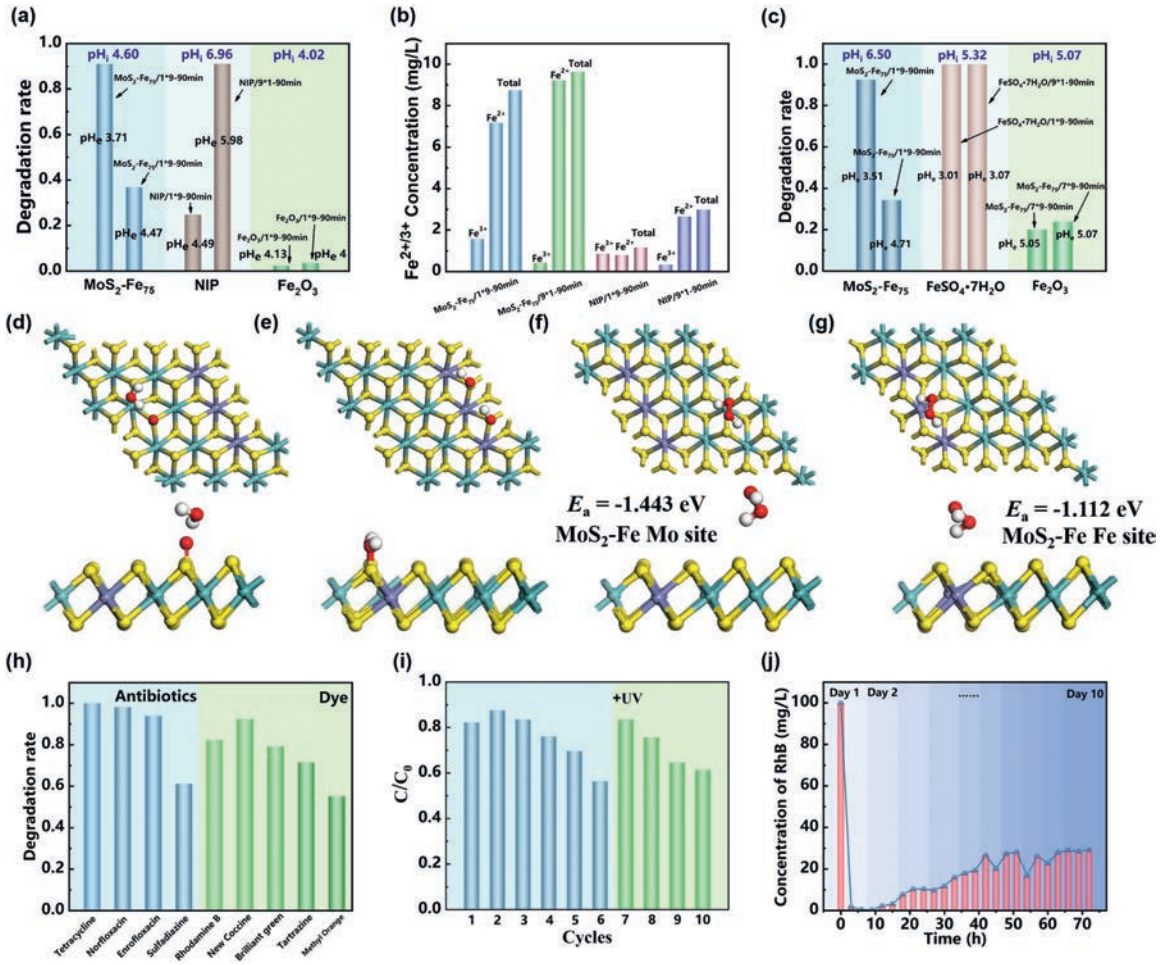


**Fig. 4.** Comparative experiments of different Fenton systems (SD: 10.0 mg/L, catalyst: 100.0 mg/L, reaction time: 90 min) and the adsorption energy of $H_2O_2$ to the surface of catalyst at different distances and degradation universality and stability test: (a) pH after adding the catalyst and its degradation effect with different $H_2O_2$ adding ways. (b) Concentration of iron ions in the solution after the reaction (pH$_i$ 4.0). (c) Comparison of homogeneous and heterogeneous Fenton systems. (d, e) The reaction of $H_2O_2$ on Mo and Fe sites of $MoS_2$-$Fe_{75}$ when $H_2O_2$ is close to the surface. (f, g) The adsorption energy of $H_2O_2$ on Mo and Fe sites of $MoS_2$-$Fe_{75}$ when $H_2O_2$ is far from the surface. (h) Degradation test for different pollutants with 100.0 mg/L $MoS_2$-$Fe_{75}$ under optimal degradation condition (Pollutant: 20.0 mg/L, $MoS_2$-$Fe_{75}$/1*9-90min for antibiotics and $MoS_2$-$Fe_{75}$/1*3-30min for dyes). (i) Cycle tests of the degradation of RhB (20.0 mg/L) in the $MoS_2$-$Fe_{75}$ + $H_2O_2$ system under the optimal conditions ($MoS_2$-$Fe_{75}$: 100.0 mg/L, $MoS_2$-$Fe_{75}$/1*3-30min). (j) 10-day continuous degradation of RhB (total concentration: 2500.0 mg/L).

dation rate of RhB maintained over 80.0% in the first 3 times with the system of $MoS_2$-$Fe_{75}$/1*3-30min and then decreased gradually. The decrease in degradation effect may be due to the degradation intermediates adsorbed on the surface of $MoS_2$-$Fe_{75}$ and this problem could be solved by UV lamp irradiation [34]. As a result, the organic intermediates on the surface of $MoS_2$-$Fe_{75}$ was further mineralized by ultraviolet light irradiation [35].

Overall, $MoS_2$-$Fe_x$ with highly dispersed iron as a novel catalyst has been successfully prepared through a simple reduction method. Specially, the $MoS_2$-$Fe_{75}$ based Fenton technology exhibits the ability to effectively degrade various organic pollutants by a "small amount for multiple times" feeding way of $H_2O_2$. In order to further verify the application prospect of the modified Fenton technology in the field of environment, we conducted a long-term degradation experiment of $MoS_2$-$Fe_{75}$/$H_2O_2$ system, as shown in Fig. 4j. When the concentration of RhB in the system was reduced from 100.0 mg/L to 30.0 mg/L or less, 100.0 mg/L of RhB was added to the reaction system to continue the reaction and the dosage of $MoS_2$-$Fe_{75}$ was 50.0 mg. In 10 days, a total of 25 times of 100.0 mg/L of RhB was added (total concentration: 2500 mg/L). The concentration of RhB in the system was reduced to 30 mg/L every time after the system of $MoS_2$-$Fe_{75}$/5*3-180min during the 10-day test. Combining with the results of the DFT calculations, when the concentration of $H_2O_2$ is low, the iron in the catalyst is not easy to directly react with $H_2O_2$, so $MoS_2$-$Fe_{75}$ has satisfactory stability when it interacts with $H_2O_2$. After drying and weighing, the weight of the remaining solid matter after the experiment is 40.5 mg and it could be calculated that 1.0 mg of RhB would be degraded for every 3.0 μL $H_2O_2$ and 0.076 mg $MoS_2$-$Fe_{75}$. This research provided a new option for overcoming the current drawbacks of Fenton reaction, including the problems of iron mud and the narrow pH range of Fenton reaction. Indeed, it provides more theoretical basis for the future application of $MoS_2$ in the various fields. By revealing the mechanism of action between $H_2O_2$ and $MoS_2$, the effect of "small amount for multiple times" $H_2O_2$ addition on Fenton activity is well explained, which has guiding significance for the future large-scale treatment of industrial wastewater by using improved Fenton technology.

## Declaration of competing interest

The authors declare that they have no known competing financial interests or personal relationships that could have appeared to influence the work reported in this paper.

## Acknowledgments

This work was supported by the State Key Research Development Program of China (No. 2016YFA0204200). Project supported by Shanghai Municipal Science and Technology Major Project (No. 2018SHZDZX03) and the Program of Introducing Talents of Discipline to Universities (No. B16017). National Natural Science Foundation of China (No. 21822603), and the Science and Technology Commission of Shanghai Municipality (No. 20DZ2250400). Authors thank Research Center of Analysis and Test of East China University of Science and Technology for the help on the characterization.

## Supplementary materials

Supplementary material associated with this article can be found, in the online version, at doi:10.1016/j.cclet.2021.08.016.

## References

[1] M. Patel, R. Kumar, K. Kishor, Chem. Rev. 119 (2019) 3510–3673.
[2] N. Chen, H. Shang, S. Tao, Environ. Sci. Technol. 52 (2018) 12656–12666.
[3] Y.H. Chuang, S. Chen, C.J. Chinn, Environ. Sci. Technol. 51 (2017) 13859–13868.
[4] Y. Yang, J.J. Pignatello, J. Ma, Environ. Sci. Technol. 48 (2014) 2344–2351.
[5] M. Du, Q. Yi, J. Ji, Chin. Chem. Lett. 31 (2020) 2803–2808.
[6] X. Lei, M. You, F. Pan, Chin. Chem. Lett. 30 (2019) 2216–2220.
[7] Y. Yin, L. Shi, W. Li, Environ. Sci. Technol. 53 (2019) 11391–11400.
[8] J. Tang, J. Wang, Environ. Sci. Technol. 52 (2018) 5367–5377.
[9] C. Wang, Y. Liu, T. Zhou, Chin. Chem. Lett. 30 (2019) 2231–2235.
[10] M. Xing, W. Xu, C. Dong, Chem. 4 (2018) 1359–1372.
[11] C. Dong, J. Ji, B. Shen, Environ. Sci. Technol. 52 (2018) 11297–11308.
[12] X. Hou, X. Huang, F. Jia, Environ. Sci. Technol. 51 (2017) 5118–5126.
[13] E. Brillas, I. Sirés, M.A. Oturan, Chem. Rev. 109 (2009) 6570–6631.
[14] J. Deng, J. Jiang, Y. Zhang, Appl. Catal. B: Environ. 84 (2008) 468–473.
[15] J. Liu, C. Dong, Y. Deng, Water Res 145 (2018) 312–320.
[16] Y. Fang, Q. Huang, P. Liu, Inorg. Chem. Front. 5 (2018) 827–834.
[17] H. Kuang, Z. He, M. Li, Chem. Eng. J. 417 (2020) 127987.
[18] K. Shen, Y. Cui, D. Zhang, J. Environ. Chem. Eng. 8 (2020) 104125.
[19] X. Yang, H. Sun, L. Zhang, Sci. Rep. 6 (2016) 1–12.
[20] L. Zhou, J. Liu, F. Dong, Spectrochim. Acta. A. Mol. Biomol. Spectrosc. 173 (2017) 544–548.
[21] W. Zhang, S. Shi, W. Zhu, Acs Appl. Mater. Inter. 9 (2017) 32720–32726.
[22] L. Gao, Q. Liao, X. Zhang, Adv. Mater. 32 (2020) 1906646.
[23] Z. Wang, W. Qiu, S.-y. Pang, Chem. Eng. J. 371 (2019) 842–847.
[24] H. Sun, G. Zhou, S. Liu, Acs Appl. Mater. Inter. 4 (2012) 6235–6241.
[25] M. Rauf, S.S. Ashraf, J. Hazard. Mater. 166 (2009) 6–16.
[26] M. Wasiewicz, A.G. Chmielewski, N. Getoff, Radiat. Phys. Chem. 75 (2006) 201–209.
[27] Q. Yi, J. Ji, B. Shen, Environ. Sci. Technol. 53 (2019) 9725–9733.
[28] J. Stencel, L. Makovsky, T. Sarkus, J. Catal. 90 (1984) 314–322.
[29] Z.-J. Niu, S.-B. Yao, S.-M. Zhou, J. Electroanal. Chem. 455 (1998) 205–207.
[30] Y. Zhu, R. Zhu, Y. Xi, Appl. Catal. B: Environ. 255 (2019) 117739.
[31] H. Zeng, L. Deng, H. Zhang, J. Hazard. Mater. 400 (2020) 123297.
[32] C. Dong, Y. Bao, T. Sheng, Appl. Catal. B: Environ. 286 (2021) 119930.
[33] L. Zhu, J. Ji, J. Liu, Angew. Chem. Int. Ed. 59 (2020) 13968–13976.
[34] J. Ji, R.M. Aleisa, H. Duan, iScience. 23 (2020) 100861.
[35] G. Matafonova, V. Batoev, Water Res. 132 (2018) 177–189.